SUPPLEMENTAL FIGURES

Figure S1 (related to Figures 1, 3, 7). Reanalysis of published single nuclei RNA-seq datasets characterizing Alzheimer's disease and age-matched non-symptomatic donors.

Figure S2 (related to Figure 1). Gating parameters for $SOX9^+$ and $LHX2^+/NeuN^-$ enrichment strategies.

Figure S3 (related to Figures 1, 3, 7). Rationale for removing D5 and D9 donors from final cohort, and general quality control metavariables for astrocytes and oligodendrocytes.

Figure S4 (related to Figure 2). Oligodendrocyte transcriptomic profiles suggest that the majority of oligodendrocytes lose critical functions in Alzheimer's disease.

Figure S5 (related to Figure 2). Sex-specific differential gene expression in oligodendrocytes.

Figure S6 (related to Figures 3, 7). Reanalysis of published single nuclei RNA-seq datasets characterizing Alzheimer's disease and age-matched non-symptomatic donors.

Figure S7 (related to Figures 3, 7). Assessment of astrocyte and oligodendrocyte donor metavariables from previously published datasets.

Figure S8 (related to Figures 3, 7). Quality control assessment of astrocyte and oligodendrocyte integrated datasets split by cluster or by dataset.

Figure S9 (related to Figure 5). Alzheimer's disease-specific GO descriptions in astrocytes.

Figure S10 (related to Figure 5). Sex-specific differential gene expression in astrocytes.

Figure S11 (related to Figures 4,5). Validation of Alzheimer's enriched astrocyte transcripts *SPARC* and *C3*.

Figure S12 (related to Figure 6). Localizing heterogeneous astrocyte gene signatures across the human and mouse cortex.

Figure S13 (related to Figures 3,7). Visualization of disease-associated transcripts from previously published datasets.

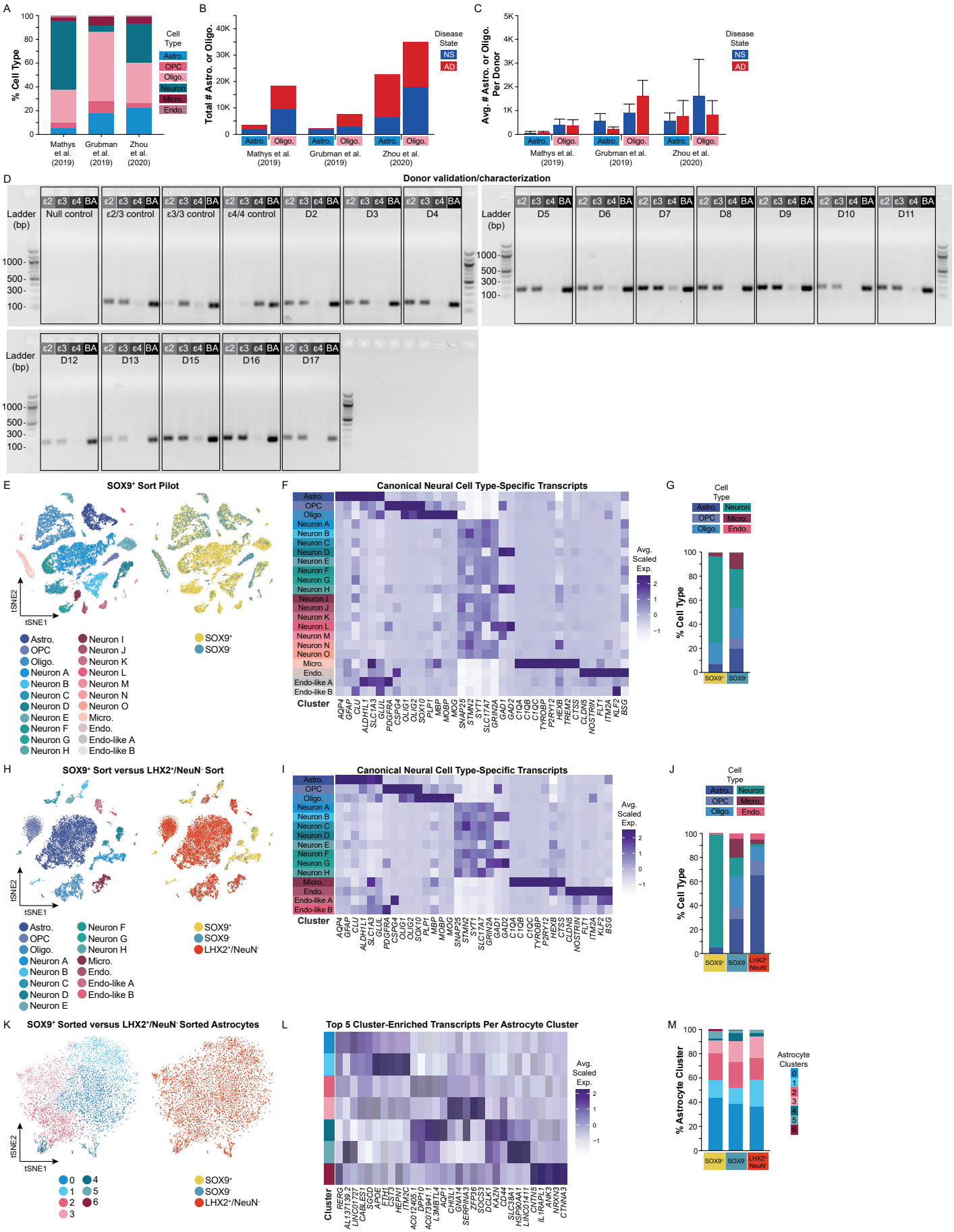
A
% Cell Type
Cell Type
Astro.
OPC
Oligo.
NeuroN
Micro.
Endo.
Mathys et al. (2019)
Grubman et al. (2019)
Zhou et al. (2020)
B
Total # Astro. or Oligo.
Disease State
NS
AD
C
Avg. # Astro. or Oligo. Per Donor
D
Donor validation/characterization
Ladder (bp)
ε2 ε3 ε4 BA
Null control
ε2/3 control
ε3/3 control
ε4/4 control
D2
D3
D4
D5
D6
D7
D8
D9
D10
D11
D12
D13
D15
D16
D17
E
SOX9⁺ Sort Pilot
tSNE1
tSNE2
SOX9⁺
SOX9⁻
F
Canonical Neural Cell Type-Specific Transcripts
Avg. Scaled Exp.
Cluster
G
% Cell Type
H
SOX9⁺ Sort versus LHX2⁺/NeuN⁻ Sort
LHX2⁺/NeuN⁻
I
J
K
SOX9⁺ Sorted versus LHX2⁺/NeuN⁻ Sorted Astrocytes
L
Top 5 Cluster-Enriched Transcripts Per Astrocyte Cluster
M
% Astrocyte Cluster
Astrocyte Clusters

Figure S1 (related to Figures 1, 3, 7). Reanalysis of published single nuclei RNA-seq datasets characterizing Alzheimer's disease and age-matched non-symptomatic donors. **(A)** Cell type proportions of total nuclei captured, **(B)** total numbers of astrocytes and oligodendrocytes captured split by disease state, and **(C)** average number of astrocytes and oligodendrocytes captured per donor split by disease state from reanalyzed snRNA-seq datasets (Mathys et al., 2019; Grubman et al., 2019; Zhou et al., 2020). **(D)** PCR confirmation of donor APOE genotype. **(E-M)** Evaluation of SOX9^{+} pilot run, and comparison of SOX9^{+} versus LHX2^{+}/NeuN^{-} sorting strategies. **(E)** tSNE plots of total nuclei (N = 18,991) captured using SOX9^{+} sorting. The tSNE plot on the left highlights all different cell types captured using this method, and the tSNE plot on the right highlights sample conditions (i.e., SOX9^{+} nuclei (N = 14,591) and SOX9^{-} nuclei (N = 4,400)). **(F)** Corresponding average scaled expression heatmap of cell type-specific transcripts **(G)** cell type proportions of nuclei captured using SOX9. **(H)** tSNE plots of total nuclei (N = 12,611) captured from a single donor using either SOX9^{+} or LHX2^{+}/NeuN^{-} sorting. The tSNE plot on the left highlights all different cell types captured, and the tSNE plot on the right highlights sample conditions (i.e., SOX9^{+} sorted nuclei (N = 2,692), SOX9^{-} sorted nuclei (N = 1,812), and LHX2^{+}/NeuN^{-} sorted nuclei (N = 8,107)). **(I)** Corresponding average scaled expression heatmap of cell type-specific transcripts by cluster and **(J)** cell type proportions of nuclei captured. **(K)** tSNE plots of only astrocytes (N = 5,918) captured from a single donor using SOX9 or LHX2^{+}/NeuN^{-}. The tSNE plot on the left highlights all astrocyte clusters, and the tSNE plot on the right highlights sample conditions (i.e., SOX9^{+} nuclei (N = 158), SOX9^{-} nuclei (N = 513), and LHX2^{+}/NeuN^{-} nuclei (N = 5,277)). **(L)** Corresponding average scaled expression heatmap of top 5 cluster enriched transcripts per cluster and **(M)** proportions of clusters captured across samples. **Abbreviations:** Astro., astrocyte; D, donor; Endo., endothelial cell; Micro., microglia; Oligo., oligodendrocyte; OPC, oligodendrocyte precursor cell.

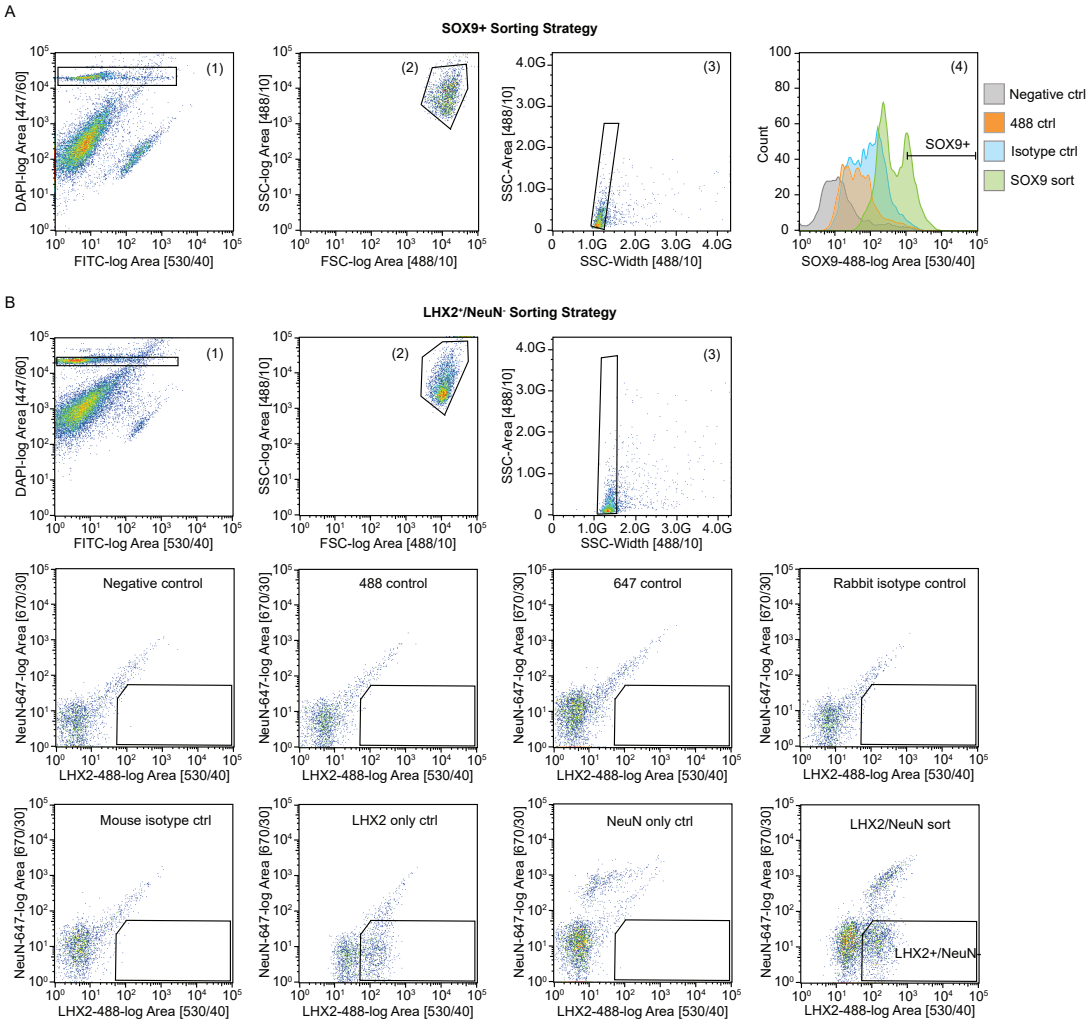

Figure S2 (related to Figure 1). Gating parameters for SOX9⁺ and LHX2⁺/NeuN⁻ enrichment strategies. **(A)** For SOX9⁺ sorting, the following gates were used to identify SOX9⁺ single nuclei: (1) Nuclei were detected using DAPI; (2) large nuclei were excluded using forward and side scatter properties; (3) doublets were excluded; and (4) SOX9⁺ nuclei were detected/collected using unlabeled (negative), secondary (488 only), and isotype controls to establish the final gate. Representative SOX9⁺ sort data are from Pilot D5. **(B)** For LHX2⁺/NeuN⁻ sorting, the following gates were used to identify LHX2⁺/NeuN⁻ single nuclei: (1) Nuclei were detected using DAPI; (2) large nuclei were excluded using forward and side scatter properties; (3) doublets were excluded; and (4) LHX2⁺/NeuN⁻ nuclei were detected/collected using unlabeled (negative), secondary (488 only and 647 only), isotype (Rabbit and Mouse), and single labeled (LHX2 only and N euN only) controls to establish the final gate. Representative LHX2⁺/NeuN⁻ sort data are from D10. **Abbreviations:** ctrl, control; DAPI, 4',6-Diamidino-2-Phenylindole Dihydrochloride; FSC, forward scatter; SSC, side scatter.

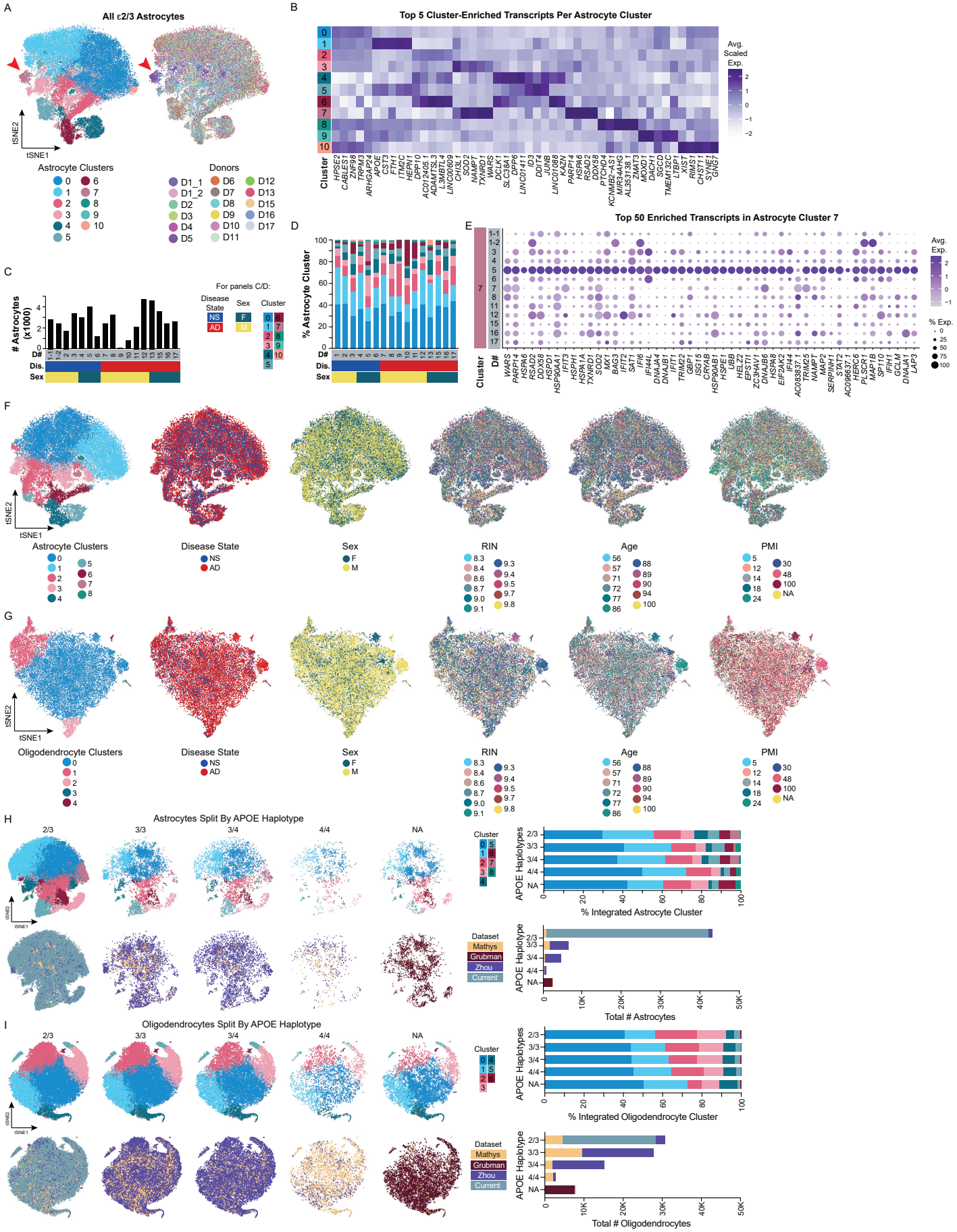
A
All ε2/3 Astrocytes
tSNE2
tSNE1
Astrocyte Clusters
0 1 2 3 4 5 6 7 8 9 10
Donors
D1_1 D1_2 D2 D3 D4 D5 D6 D7 D8 D9 D10 D11 D12 D13 D15 D16 D17
B
Top 5 Cluster-Enriched Transcripts Per Astrocyte Cluster
Avg. Scaled Exp.
Cluster
HPSE2 CABLES1 PDE4B TRPM3 ARHGAP24 APOE CST3 FTH1 HMGCS1 HEPACAM DPP10 AC012405.1 ADAMTSL3 L3MBTL4 LINC00609 CHI3L1 SOD2 NAMPT TXNRD1 WARS DCLK1 SLC38A1 DTYMK LINC01411 ID3 DDIT4 JUNB LINC01088 KAZN PARP14 HSPA6 RSAD2 DDX58 PTCHD4 KCNMB2-AS1 MIR34AHG AL353138.3 ZNF41 MOXD1 DACH1 SGCD TMEM132C LTBP1 KIF1A RMST CHST11 SYNE1 GNG7
C
Astrocytes (x1000)
D#
Dis.
Sex
For panels C/D:
Disease State NS AD
Sex F M
Cluster
D
% Astrocyte Cluster
E
Top 50 Enriched Transcripts in Astrocyte Cluster 7
Avg. Exp.
% Exp.
WARS PARP14 HSPA6 RSAD2 DDX58 HSPD1 HSP90AA1 IFIT3 HSPH1 HSPA1A TXNRD1 SOD2 MX1 BAG3 IFIT2 SAT1 IFI6 IFI44L DNAJA4 DNAJB1 IFIT1 TRIM22 GBP1 ISG15 CRYAB HSP90AB1 HSPE1 HSPB1 HELZ2 EPSTI1 ZC3HAV1 DNAJB6 HSPA8 EIF2AK2 IFI44 AC018362.1 TRIM25 NAMPT MAP2 SERPINH1 STAT2 AC099637.1 HERC6 PLSCR1 MAP1B SP110 IFIH1 GCLM DNAJA1 LAP3
F
tSNE2
tSNE1
Astrocyte Clusters
0 1 2 3 4 5 6 7 8
Disease State
NS AD
Sex
F M
RIN
8.3 8.4 8.6 8.7 9.0 9.1 9.3 9.4 9.5 9.7 9.8
Age
56 57 71 72 77 86 88 89 90 94 100
PMI
5 12 14 18 24 30 48 100 NA
G
tSNE2
tSNE1
Oligodendrocyte Clusters
0 1 2 3 4
Disease State
NS AD
Sex
F M
RIN
8.3 8.4 8.6 8.7 9.0 9.1 9.3 9.4 9.5 9.7 9.8
Age
56 57 71 72 77 86 88 89 90 94 100
PMI
5 12 14 18 24 30 48 100 NA
H
Astrocytes Split By APOE Haplotype
2/3 3/3 3/4 4/4 NA
tSNE2
tSNE1
Cluster
0 5 1 6 2 7 3 8 4
Dataset
Mathys Grubman Zhou Current
APOE Haplotypes
% Integrated Astrocyte Cluster
Total # Astrocytes
I
Oligodendrocytes Split By APOE Haplotype
2/3 3/3 3/4 4/4 NA
tSNE2
tSNE1
Cluster
0 4 1 5 2 6 3
Dataset
Mathys Grubman Zhou Current
APOE Haplotypes
% Integrated Oligodendrocyte Cluster
Total # Oligodendrocytes

Figure S3 (related to Figures 1, 3, 7). Rationale for removing D5 and D9 donors from final cohort, and general quality control metavariables for astrocytes and oligodendrocytes. **(A)** tSNE plots of astrocyte nuclei (N = 45,088) captured from all 16 donors using $LHX2^{+}/NeuN^{-}$. The tSNE plot on the left highlights all astrocyte clusters, and the tSNE plot on the right highlights donor contribution across clusters. It is clear that D5 drives a single cluster (cluster 7, arrows) and as such these sequencing data were removed from downstream processing. **(B)** Corresponding average scaled expression heatmap of top 5 enriched/unique transcripts per astrocyte cluster. **(C)** Total number of astrocytes identified per donor post-quality check analysis. Donor 9 was excluded from downstream analysis due to low number of astrocytes identified (116 astrocytes). Additional donor metavariables highlighted include disease state (blue, NS donors; red, AD donors) and sex (green, female; yellow, male). **(D)** Proportion of astrocyte clusters identified in each donor. Additional metavariables highlighted described in panel F. **(E)** Dotplot of top 50 enriched transcripts in cluster 7 astrocytes split by donor. NB. Cluster 7 was driven by a single donor (D5). **(F,G)** Donor sample metavariables - tSNE plots of (from left to right) uniquely defined clusters, RNA quality of donor samples, age range of donors, and post-mortem interval of donor samples for **(F)** captured astrocytes (N = 41,071) and **(G)** oligodendrocytes (N = 23,840). Ages are listed in years, and PMIs in hours. **(H,I)** tSNE plots and total capture rate/percentage capture for astrocytes **(H)** and oligodendrocytes **(I)** across donors (see **Figures S6, S7**). tSNE plots show no cluster was driven specifically by *APOE* genotype, thought capture rates for *APOE* 3/3, 3/4, and 4/4 donors are much lower than for *APOE* 2/3 donors used in the current study. **Abbreviations:** AD, Alzheimer's disease; D#, donor number; Dis., disease state; F, female; M, male; NA, not applicable as no information was available from brain bank; NS, non-symptomatic. PMI, Post-Mortem Interval; RIN, RNA Integrity Number.

A

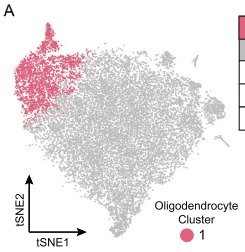

CLUSTER 1 UNIQUE UPREGULATED GO TERMS			
GO term	Description	GO term	Description
GO:0050770	Regulation of axonogenesis	GO:0016358	Dendrite development
GO:0007409	Axonogenesis	GO:1905874	Reg. of postsynaptic density organization
GO:1901626	Reg. of postsynaptic membrane organization	GO:0001941	Postsynaptic membrane organization

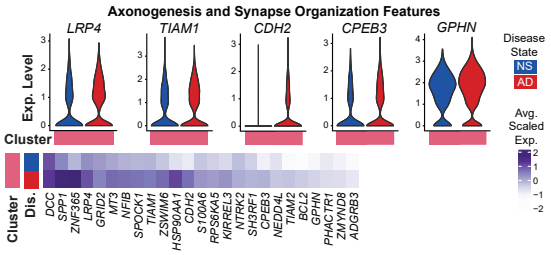

B

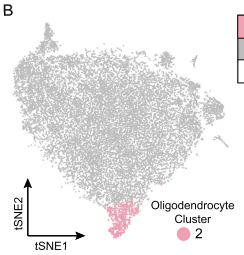

CLUSTER 2 UNIQUE UPREGULATED GO TERMS	
GO term	Description
GO:0090181	Regulation of cholesterol metabolic process

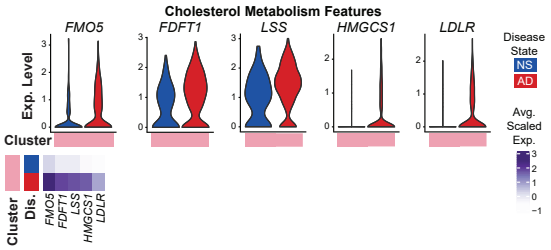

C

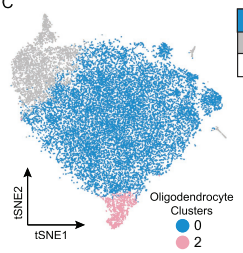

CLUSTERS 0/2 UPREGULATED GO TERMS	
GO term	Description
GO:0051056	Regulation of small GTPase mediated signal transduction

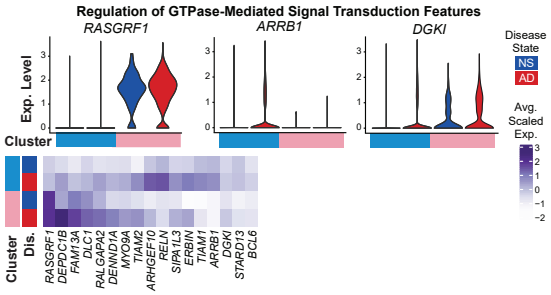

CLUSTERS 0/2 DOWNREGULATED GO TERMS			
GO term	Description	GO term	Description
GO:0046394	Carboxylic acid biosynthesis process	GO:0008652	Cellular amino acid biosynthetic process
GO:0016053	Organic acid biosynthetic process		

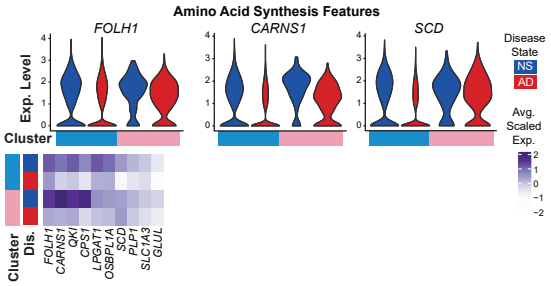

D

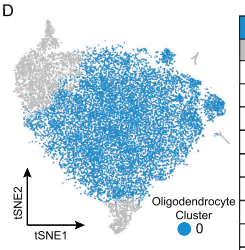

CLUSTER 0 UNIQUE DOWNREGULATED GO TERMS*			
GO term	Description	GO term	Description
GO:0050804	Modulation of chemical synaptic transmission	GO:0001941	Postsynaptic membrane organization
GO:0099177	Regulation of trans-synaptic signaling	GO:0098917	Retrograde trans-synaptic signaling
GO:0042391	Regulation of membrane potential	GO:0097104	Postsynaptic membrane assembly
GO:0050806	Positive regulation of synaptic transmission	GO:0098693	Regulation of synaptic vesicle cycle
GO:0035249	Synaptic transmission, glutamatergic	GO:2000302	Pos. reg. of synaptic vesicle exocytosis
GO:0060078	Reg. of postsynaptic membrane potential	GO:0099003	Vesicle-mediated transport in synapse
GO:0050773	Regulation of dendrite development	GO:0016079	Synaptic vesicle exocytosis
GO:0050808	Synapse organization	GO:0006836	Neurotransmitter transport
GO:0007215	Glutamate receptor signaling pathway	GO:0001505	Regulation of neurotransmitter levels
GO:0043113	Receptor clustering	GO:0001956	Pos. reg. of neuro-transmitter secretion
GO:0060079	Excitatory postsynaptic potential	GO:0032412	Reg. of ion transmem. transporter activity
GO:0099175	Regulation of post-synapse organization	GO:2001257	Regulation of cation channel activity
GO:0099643	Signal release from synapse	GO:1904062	Regulation of cation transmem. transport
GO:0048167	Regulation of synaptic plasticity	GO:0071805	Postassium ion transmem. transport

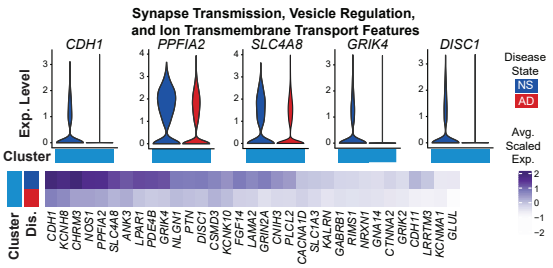

CLUSTER 0 UNIQUE DOWNREGULATED GO TERMS			
GO term	Description	GO term	Description
GO:0009214	Cyclic nucleotide catabolic process	GO:0006195	Purine nucleotide catabolic process
GO:0009187	Cyclic nucleotide metabolic process	GO:0046068	cGMP metabolic process
GO:0009154	Purine ribonucleotide catabolic process	GO:0072523	Purine-containing comp. catabolic process
GO:0009261	Ribonucleotide catabolic process	GO:0046058	cAMP metabolic process
GO:0009166	Nucleotide catabolic process	GO:0046434	Organophosphate catabolic process
GO:1901292	Nucleotside phosphate catabolic process		

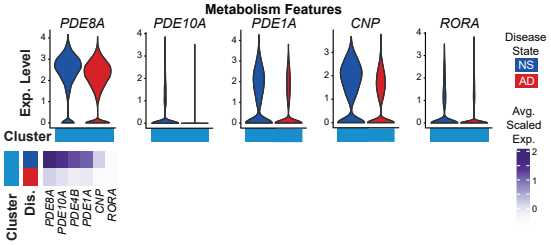

Figure S4 (related to Figure 2). Oligodendrocyte transcriptomic profiles suggest that the majority of oligodendrocytes have altered critical functions in Alzheimer's disease. tSNE plots highlighting clusters of interest, unique/shared GO terms, and differentially expressed genes (DEGs) associated with GO terms. GO-associated DEGs are plotted as average scaled expression heatmaps by cluster(s) of interest and split by disease state (blue, NS donors; red, AD donors). Additionally, example DEG violin plots to resolve the range of expression (log normalized UMI counts) across all oligodendrocytes in single or multiple clusters. **(A)** Upregulated axonogenesis and synapse organization features unique to cluster 1. **(B)** Upregulated cholesterol metabolism features unique to cluster 2. **(C)** Upregulated regulation of GTPase-mediated signal transduction features and downregulated amino acid synthesis features shared by clusters 0 and 2. **(D)** Downregulated synapse transmission, vesicle regulation, and ion transmembrane transport features as well as downregulated metabolism features unique to cluster 0. **Abbreviations:** AD, Alzheimer's disease; Comp., compound; DEG, differentially expressed genes; Dep., dependent; Dis., disease; GO, gene ontology; NS, non-symptomatic; Pos., positive; Reg., regulation; Transmem., transmembrane; UMI, unique molecular identifier.

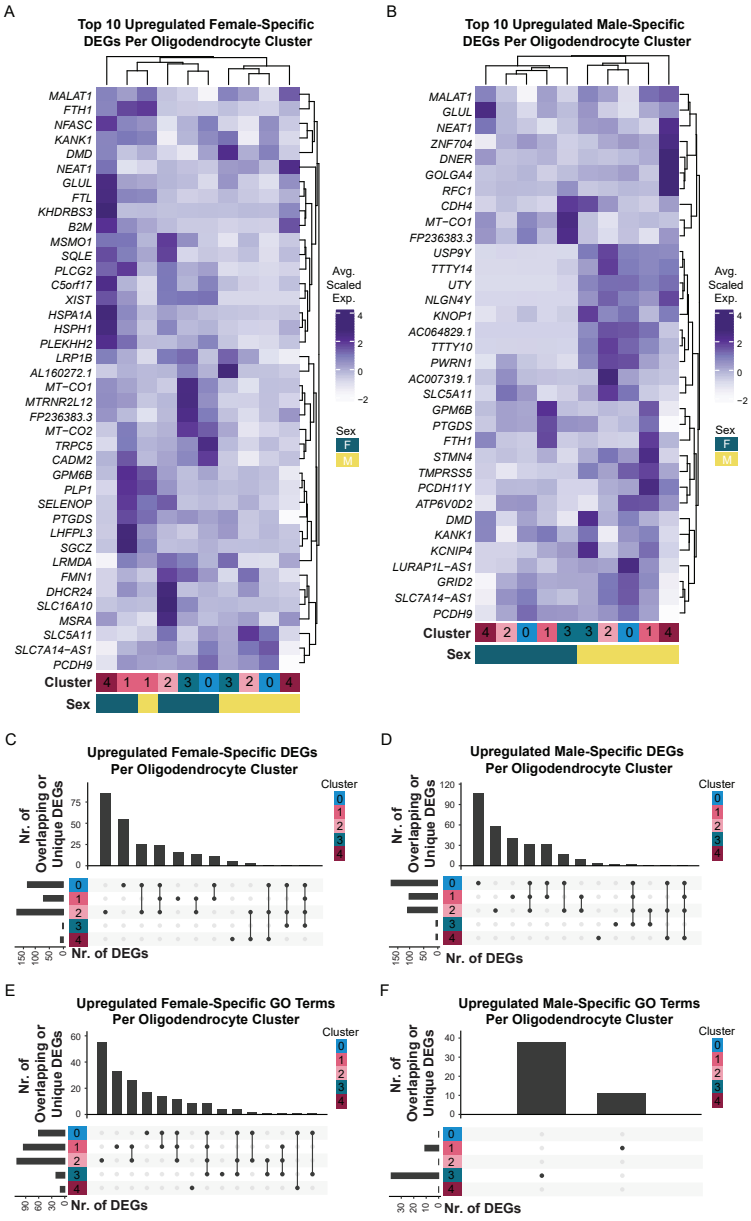

Figure S5 (related to Figure 2). Sex-specific differential gene expression in oligodendrocytes. Up- and down-regulated female **(A)** and male **(B)** transcripts split by oligodendrocyte cluster. **(C-F)** UpSetR plots highlighting sex-specific upregulated DEGs or GO terms that are unique to or shared between oligodendrocyte clusters. **Abbreviations:** DEG, differentially expressed gene; F, female; GO, gene ontology; M, male.

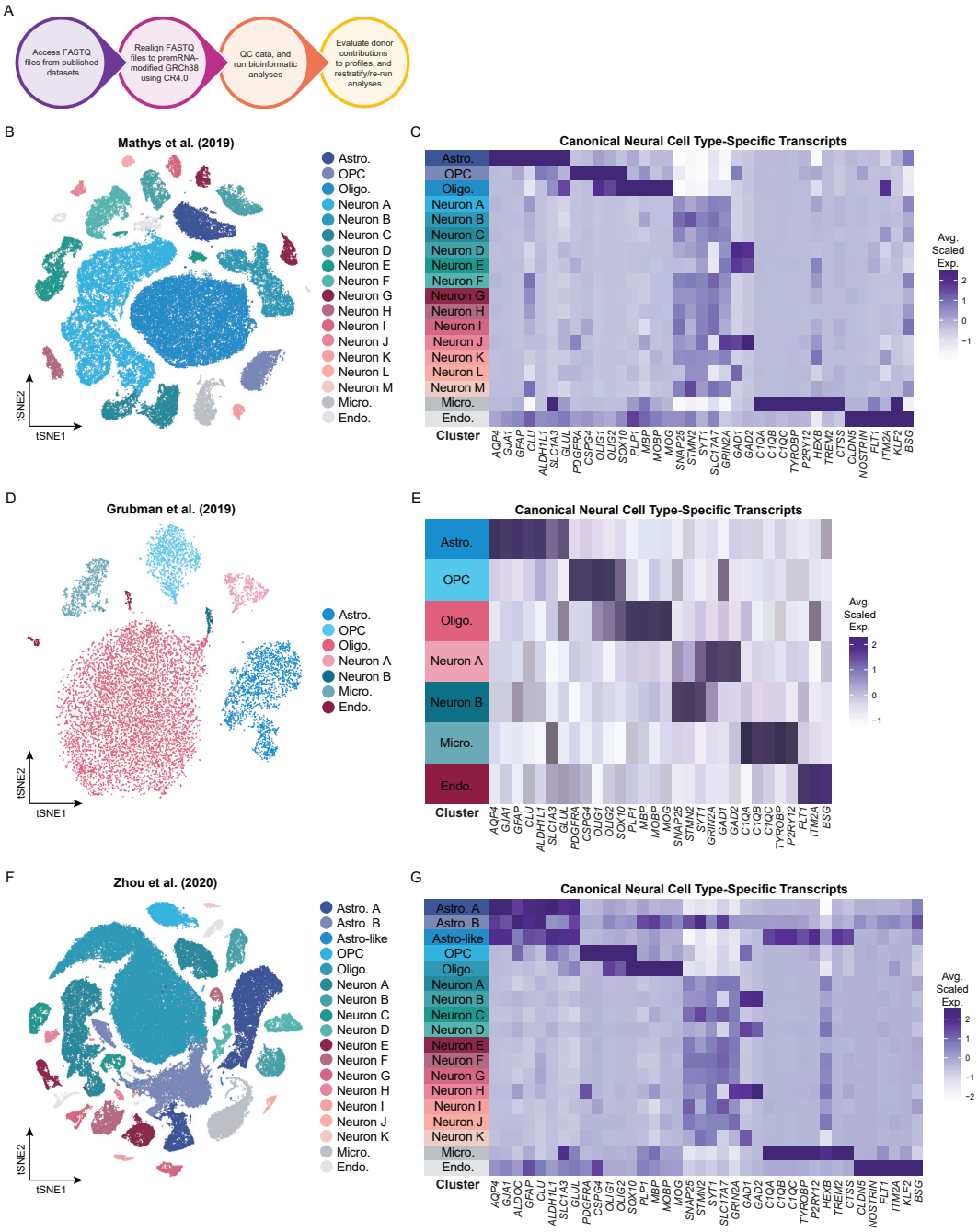

Figure S6 (related to Figures 3, 7). Reanalysis of published single nuclei RNA-seq datasets characterizing Alzheimer's disease and age-matched non-symptomatic donors. **(A)** Work process overview for data reanalysis: realigning original FASTQ files to the same premRNA modified GRCh38 human reference genome using the same version of Cell Ranger software (v4.0.0), and running quality control/all downstream analyses. Datasets reanalyzed included Mathys et al. (2019) **(B-C)**, Grubman et al. (2019) **(D-E)**, and Zhou et al. (2020) **(F-G)**. For each dataset, tSNE plots of all captured nuclei (Mathys N = 64,909; Grubman N = 13,095; Zhou N = 101,383), and clusters defined based on ability to detect transcriptomically unique features **(B, D, F)**. By evaluating the averaged scaled expression of cell type-specific features in each cluster **(C, E, G)**, cell type identities were assigned post-hoc to each respective cluster. **Abbreviations:** Astro., astrocyte; CR, Cell Ranger software (version 4.0.0); Endo., endothelial cell; Micro., microglia; Oligo., oligodendrocyte; OPC, oligodendrocyte precursor cell.

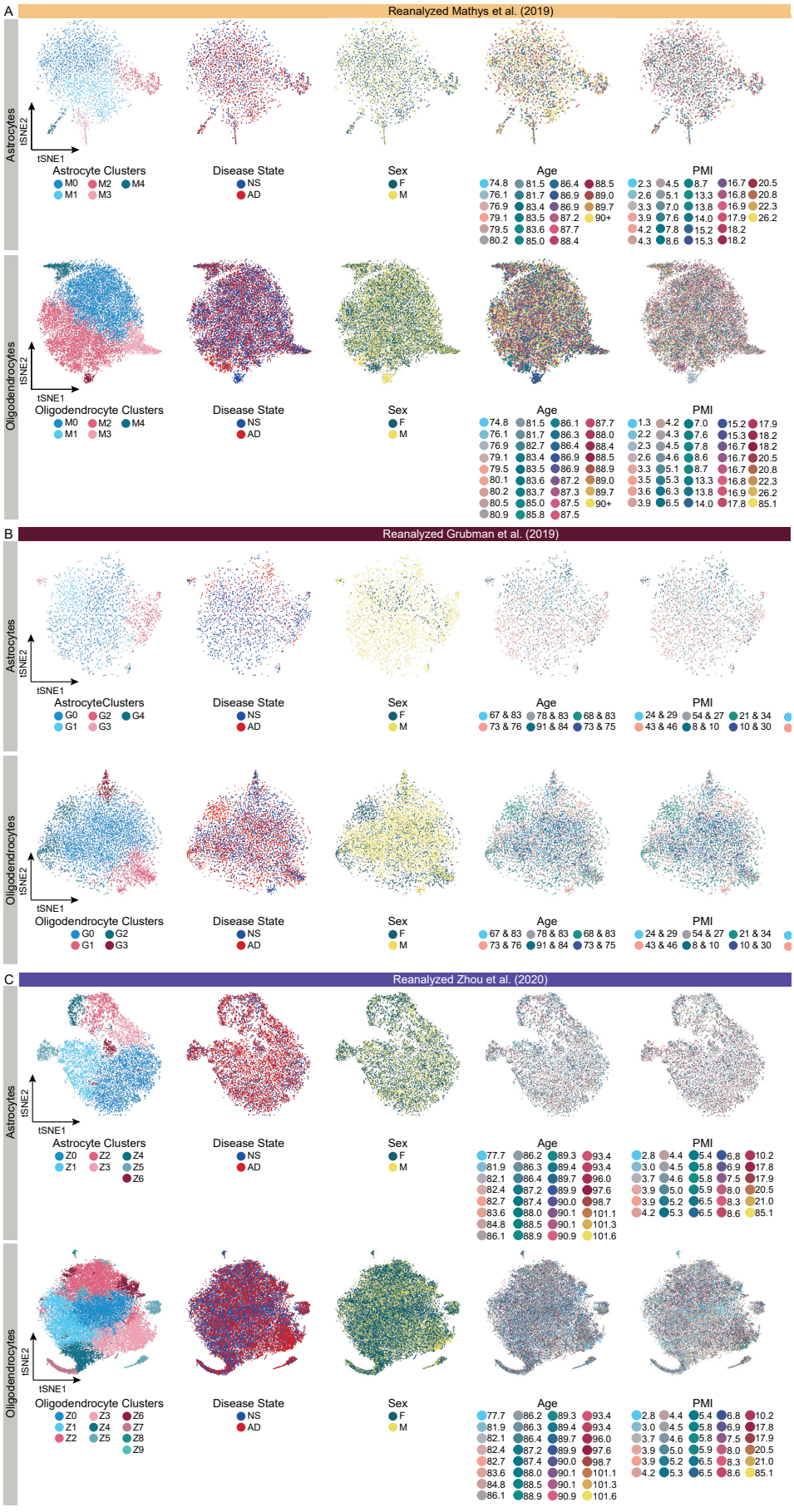
A
Reanalyzed Mathys et al. (2019)
Astrocytes
tSNE2
tSNE1
Astrocyte Clusters
M0 M2 M4
M1 M3
Disease State
NS
AD
Sex
F
M
Age
74.8 81.5 86.4 88.5
76.1 81.7 86.9 89.0
76.9 83.4 86.9 89.7
79.1 83.5 87.2 90+
79.5 83.6 87.7
80.2 85.0 88.4
PMI
2.3 4.5 8.7 16.7 20.5
2.6 5.1 13.3 16.8 20.8
3.3 7.0 13.8 16.9 22.3
3.9 7.6 14.0 17.9 26.2
4.2 7.8 15.2 18.2
4.3 8.6 15.3 18.2
Oligodendrocytes
tSNE2
tSNE1
Oligodendrocyte Clusters
M0 M2 M4
M1 M3
Disease State
NS
AD
Sex
F
M
Age
74.8 81.5 86.1 87.7
76.1 81.7 86.3 88.0
76.9 82.7 86.4 88.4
79.1 83.4 86.9 88.5
79.5 83.5 86.9 88.9
80.1 83.6 87.2 89.0
80.2 83.7 87.3 89.7
80.5 85.0 87.5 90+
80.9 85.8 87.5
PMI
1.3 4.2 7.0 15.2 17.9
2.2 4.3 7.6 15.3 18.2
2.3 4.5 7.8 16.7 18.2
2.6 4.6 8.6 16.7 20.5
3.3 5.1 8.7 16.7 20.8
3.5 5.3 13.3 16.8 22.3
3.6 6.3 13.8 16.9 26.2
3.9 6.5 14.0 17.8 85.1
B
Reanalyzed Grubman et al. (2019)
Astrocytes
tSNE2
tSNE1
AstrocyteClusters
G0 G2 G4
G1 G3
Disease State
NS
AD
Sex
F
M
Age
67 & 83 78 & 83 68 & 83
73 & 76 91 & 84 73 & 75
PMI
24 & 29 54 & 27 21 & 34
43 & 46 8 & 10 10 & 30
Oligodendrocytes
tSNE2
tSNE1
Oligodendrocyte Clusters
G0 G2
G1 G3
Disease State
NS
AD
Sex
F
M
Age
67 & 83 78 & 83 68 & 83
73 & 76 91 & 84 73 & 75
PMI
24 & 29 54 & 27 21 & 34
43 & 46 8 & 10 10 & 30
C
Reanalyzed Zhou et al. (2020)
Astrocytes
tSNE2
tSNE1
Astrocyte Clusters
Z0 Z2 Z4
Z1 Z3 Z5
Z6
Disease State
NS
AD
Sex
F
M
Age
77.7 86.2 89.3 93.4
81.9 86.3 89.4 93.4
82.1 86.4 89.7 96.0
82.4 87.2 89.9 97.6
82.7 87.4 90.0 98.7
83.6 88.0 90.1 101.1
84.8 88.5 90.1 101.3
86.1 88.9 90.9 101.6
PMI
2.8 4.4 5.4 6.8 10.2
3.0 4.5 5.8 6.9 17.8
3.7 4.6 5.8 7.5 17.9
3.9 5.0 5.9 8.0 20.5
3.9 5.2 6.5 8.3 21.0
4.2 5.3 6.5 8.6 85.1
Oligodendrocytes
tSNE2
tSNE1
Oligodendrocyte Clusters
Z0 Z3 Z6
Z1 Z4 Z7
Z2 Z5 Z8
Z9
Disease State
NS
AD
Sex
F
M
Age
77.7 86.2 89.3 93.4
81.9 86.3 89.4 93.4
82.1 86.4 89.7 96.0
82.4 87.2 89.9 97.6
82.7 87.4 90.0 98.7
83.6 88.0 90.1 101.1
84.8 88.5 90.1 101.3
86.1 88.9 90.9 101.6
PMI
2.8 4.4 5.4 6.8 10.2
3.0 4.5 5.8 6.9 17.8
3.7 4.6 5.8 7.5 17.9
3.9 5.0 5.9 8.0 20.5
3.9 5.2 6.5 8.3 21.0
4.2 5.3 6.5 8.6 85.1

Figure S7 (related to Figures 3, 7). Assessment of astrocyte and oligodendrocyte donor metavariables from previously published datasets. tSNE plots of (from left to right) uniquely defined clusters, disease state, sex, age range of donors, post-mortem interval, and APOE genotype of donors for **(A)** Mathys et al. (2019) astrocytes (N = 3,079) and oligodendrocytes (N = 18,229), **(B)** Grubman et al. (2019) astrocytes. (N = 2,330) and oligodendrocytes (N = 7,604), and **(C)** Zhou et al. (2020) astrocytes (N = 10,538) and oligodendrocytes (N = 34,949). Ages are listed in years, and PMIs in hours. **Abbreviations:** AD, Alzheimer's disease; NA, not applicable as no information was available from published manuscript; NS, non-symptomatic; PMI, Post-Mortem Interval; RIN, RNA Integrity Number.

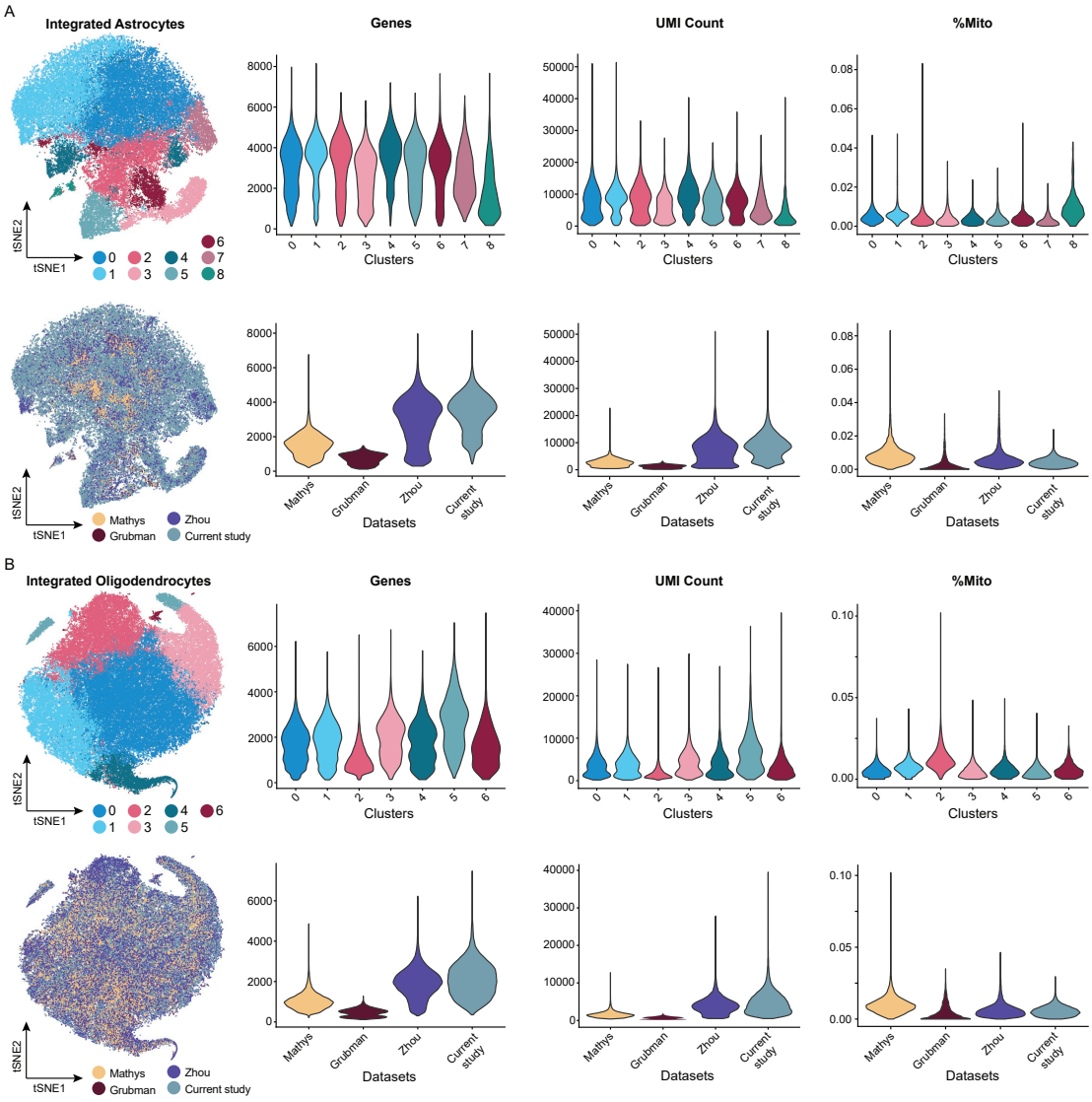

Figure S8 (related to Figures 3, 7). Quality control assessment of astrocyte and oligodendrocyte integrated datasets split by cluster or by dataset. tSNE plots of integrated **(A)** astrocytes (N = 57,018) and **(B)** oligodendrocytes (N = 84,622) as visualized by cluster (top) and by dataset (bottom). Representative violin plots of the number of genes captured per nucleus ("Genes"), the number of UMIs counted per nucleus ("UMI Count"), and the percentage of mitochondrial DNA contamination ("%Mito"). Mathys et al. (2019) data are in yellow, Grubman et al. (2019) data are in dark red, Zhou et al. (2020) data are in violet, and the current study's data are in steel blue. **Abbreviations:** %Mito, percentage of mitochondrial DNA contamination; UMI, unique molecular identifier.

A

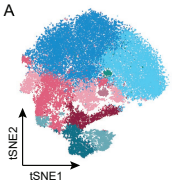

Astrocyte Clusters: 0 5 1 6 2 7 3 8 4

Disease State: NS, AD

Cluster(s)	Upregulated Disease-Specific GO Description	Cluster(s)	Upregulated Disease-Specific GO Description
0	Response to steroids/hormones	5	Lipid storage/ Fatty acid oxidation/ Response to steroids
1	Cell death / Oxidative stress	6	Apoptotic signaling/ Response to stress
2	Lipid localization	0/1 /4/6	Response to metal ions
3	Cytoskeletal organization/ Synaptic structure	1/3/4	Synaptic organization and signaling
4	Cell-matrix adhesion	4/ 6	Protein folding and unfolding

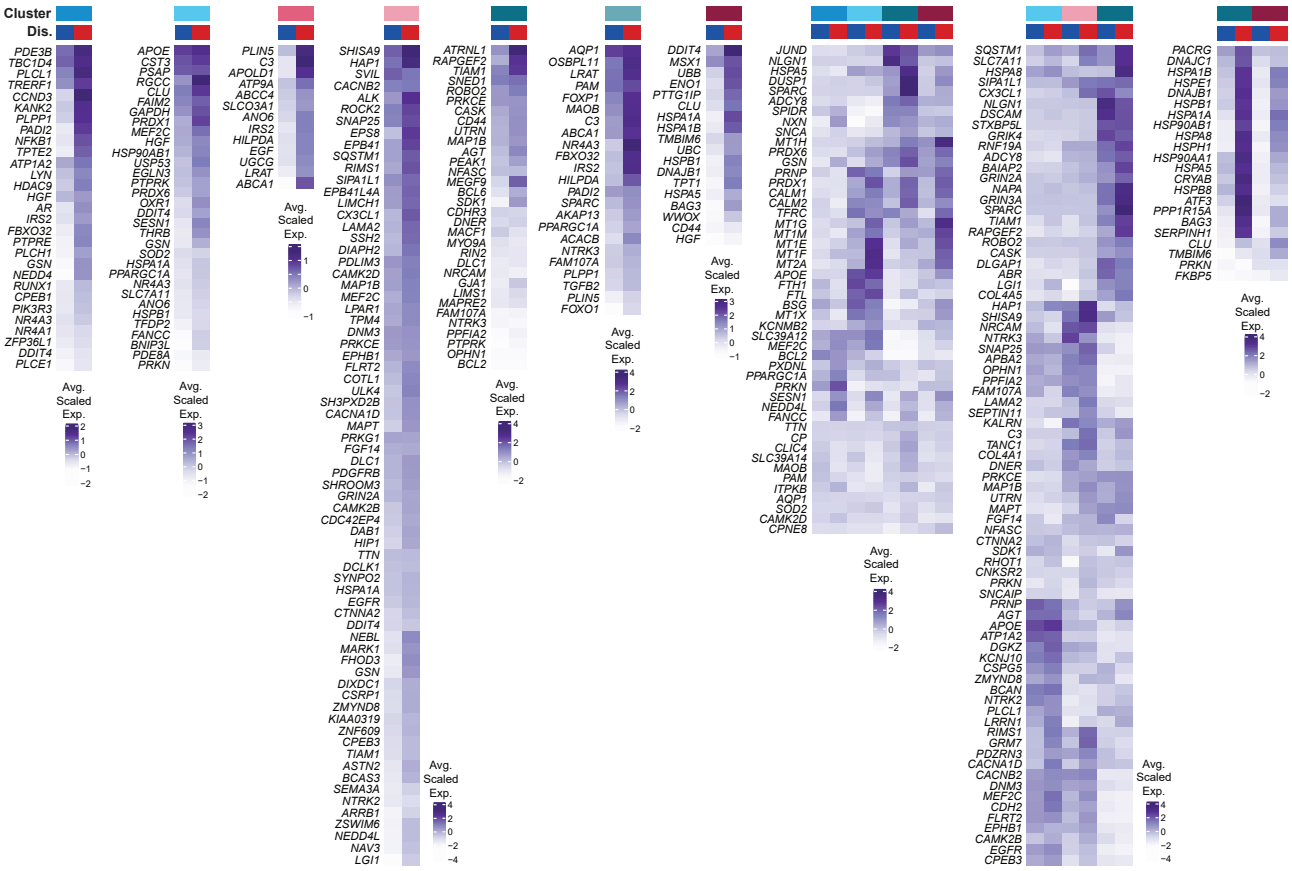

B

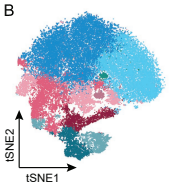

Astrocyte Clusters: 0 5 1 6 2 7 3 8 4

Disease State: NS, AD

Cluster	Downregulated Disease-Specific GO Description	Clusters	Downregulated Disease-Specific GO Description
2	Glial cell differentiation	2/3/5/7	Response to metal ions
3	Angiogenesis regulation/ BBB maintenance	2/4/5/6	Synaptic organization and transmission
4	Axon and synapse regulation*	4/ 6	Signaling receptor activity and axonal guidance
5	ERK1/2 cascade signaling		

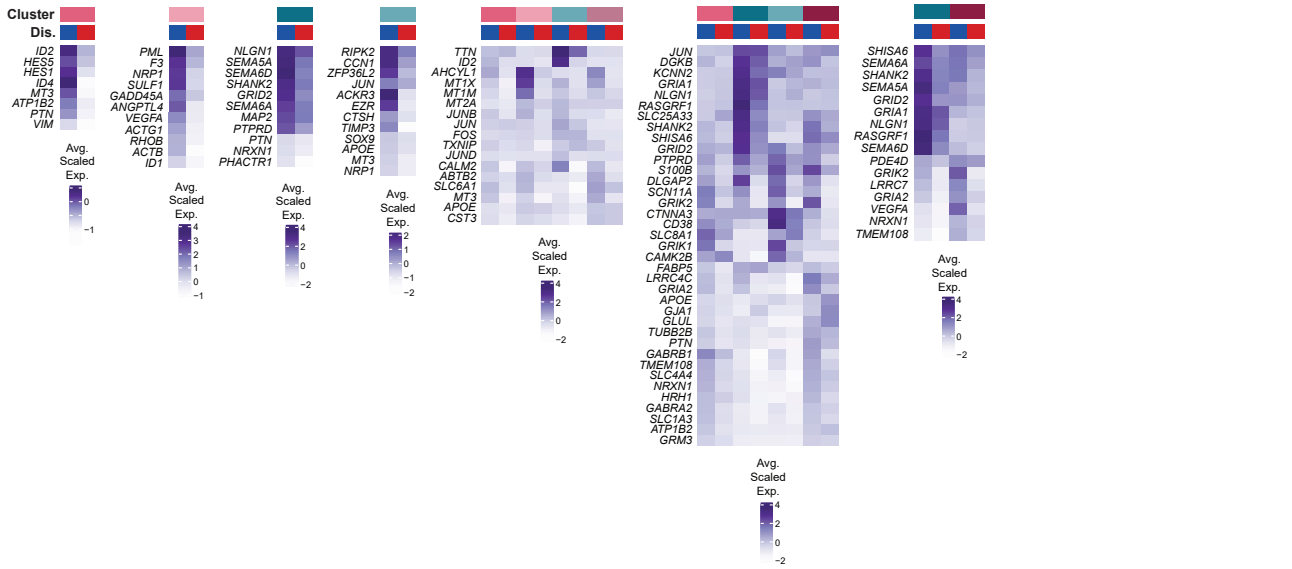

Figure S9 (related to Figure 5). Alzheimer's disease-specific GO descriptions in astrocytes. **(A)** Table lists summarized key upregulated GO descriptions (i.e., manual curation and summation of multiple identified GO terms) unique to single astrocyte clusters as well as GO descriptions that are shared by multiple clusters. Differentially expressed genes (DEGs) associated with these GO descriptions are listed on each heatmap for respective clusters (color coding key listed on the top right). Average scaled expression of DEGs are visualized comparing astrocytes isolated from non-symptomatic (blue) and Alzheimer's disease (red) donors. **(B)** Table lists summarized key downregulated GO descriptions (i.e., manual curation and summation of multiple identified GO terms) unique to single clusters as well as GO descriptions that are shared by multiple clusters. Differentially expressed genes (DEGs) associated with these GO descriptions are listed on each heatmap for respective clusters (color coding key listed on the top right). Average scaled expression of DEGs are visualized comparing astrocytes isolated from non-symptomatic (blue) and Alzheimer's disease (red) donors. **Abbreviations:** AD, Alzheimer's disease; BBB, blood brain barrier; Dis., disease state; GO, gene ontology; NS, non-symptomatic.

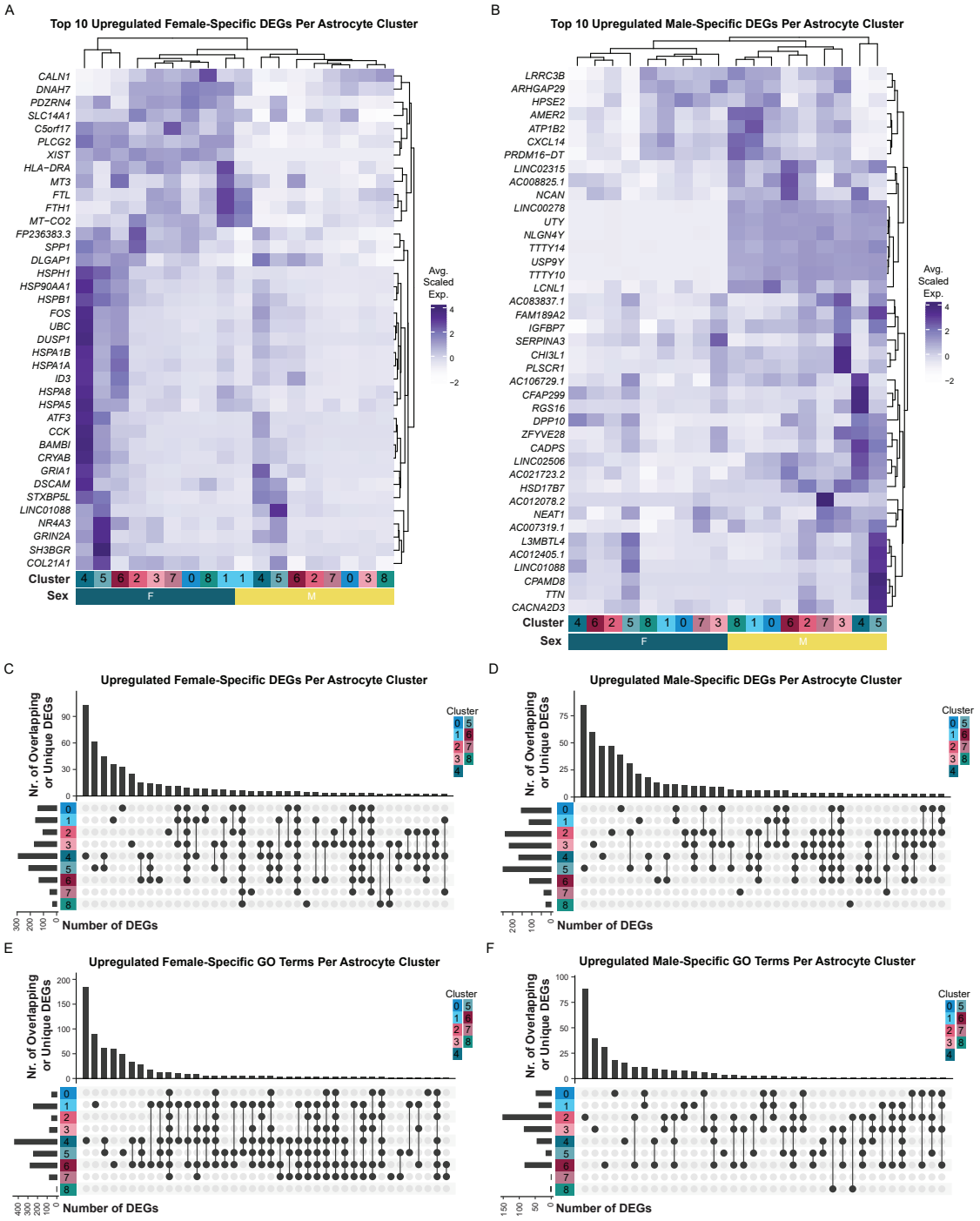

Figure S10 (related to Figure 5). Sex-specific differential gene expression in astrocytes. Up- and down-regulated female **(A)** and male **(B)** transcripts split by astrocyte cluster. (C-F) UpSetR plots highlighting sex-specific upregulated DEGs or GO terms that are unique to or shared between astrocyte clusters. **Abbreviations:** DEG, differentially expressed gene; F, female; GO, gene ontology; M, male.

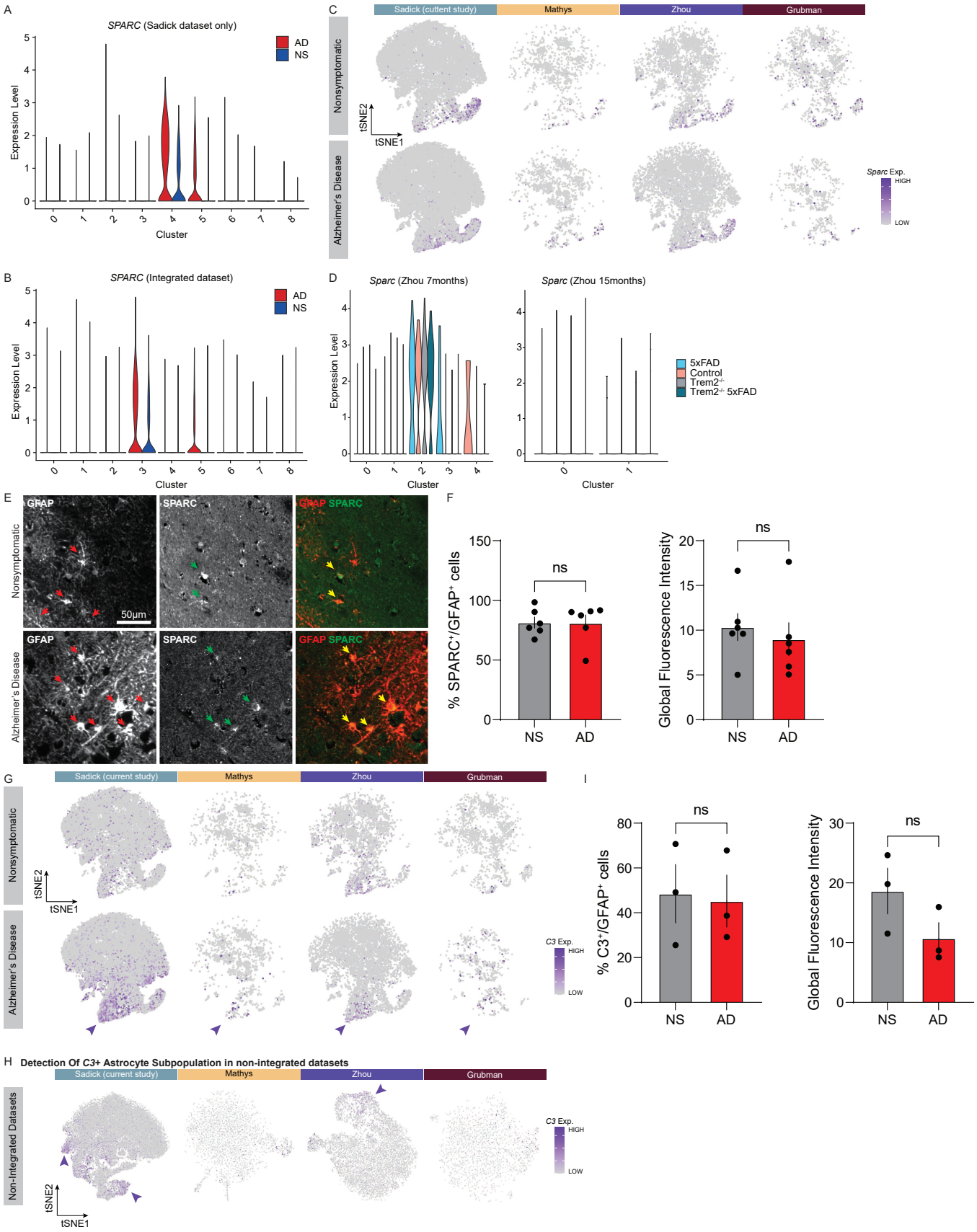

Figure S11 (related to Figures 4,5). Validation of Alzheimer's enriched astrocyte transcripts *SPARC* and *C3*. **(A)** Violin plot highlighting cluster-specific and Alzheimer's disease (AD) enrichment in expression of *SPARC* in clusters 4 and 5 in the current dataset. **(B)** This enrichment of *SPARC* was maintained across the integrated datasets. **(C)** Feature plots from the integrated dataset, split per dataset highlighting expression of *SPARC* in astrocytes, and enrichment in AD donor samples. **(D)** Violin plot of Zhou et al (2020) data

from wildtype control, *5xFAD*, *Trem2*$^{-/-}$, and *5xFAD*/*Trem2*$^{-/-}$ mice highlights enrichment of *Sparc* in astrocytes at 7 months (early) by not 15 months (late timepoints) in a mouse model of AD. **(E)** Immunofluorescent validation of SPARC in non-symptomatic (top) and human AD (bottom) tissue, co-localized with the astrocyte marker GFAP. **(F)** Quantification of the percentage of SPARC^{+} astrocytes and global fluorescence intensity for SPARC across six separate donors. **(G)** Feature plots from the integrated dataset, split per dataset, highlighting expression of *C3* in astrocytes, and enriched in AD donor samples. Arrows highlight *C3*$^{+}$ clusters. *C3*$^{+}$ cells were not detected in the Mathys (2019) or Grubman (2019) datasets prior to integration **(H)** due to low capture rates of astrocytes. **(I)** Quantification of C3+ cells as a proportion of GFAP+ astrocytes using immunofluorescence. Raw quantification values are displayed as well as mean ± s.e.m. in panels F and I.

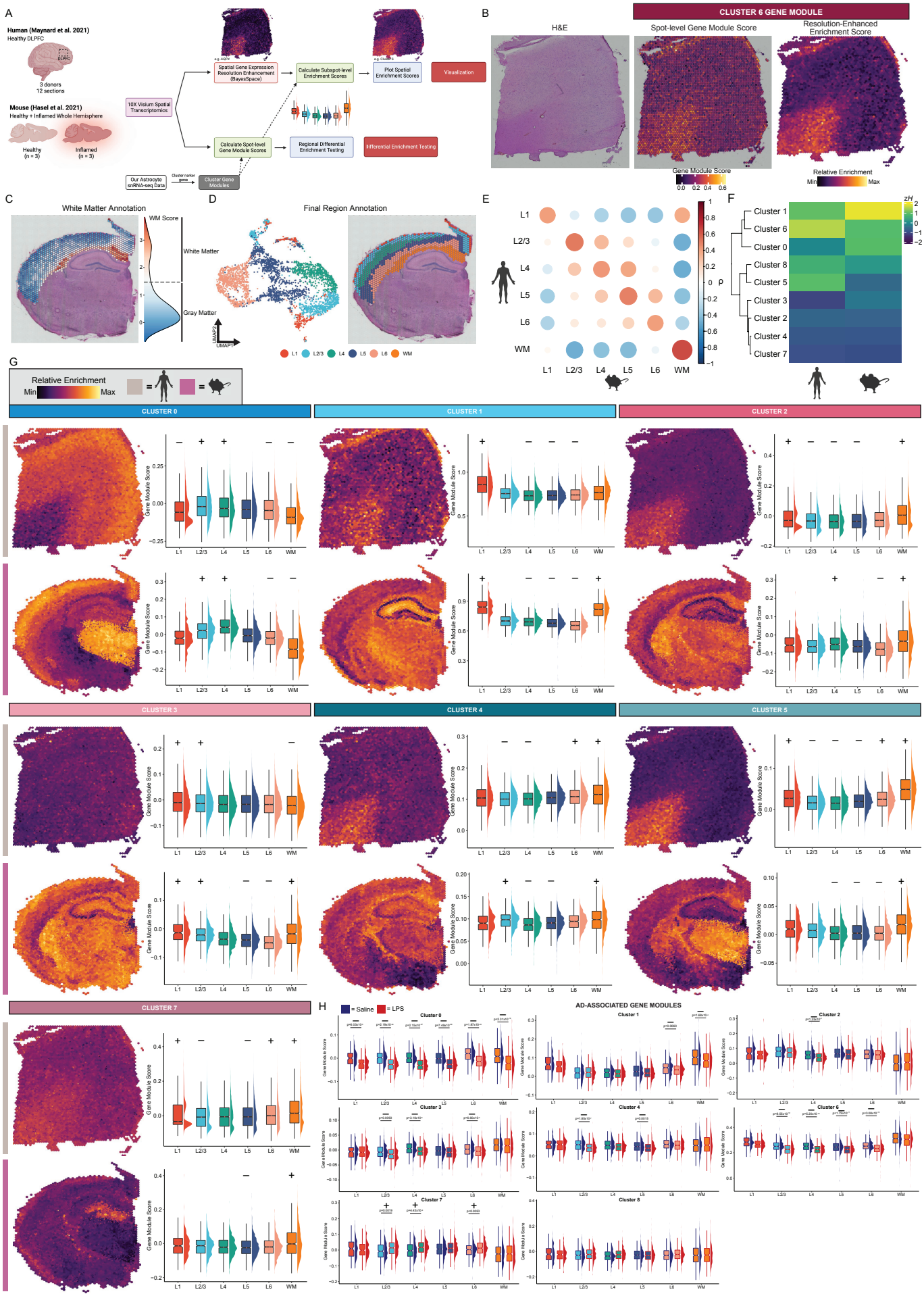
A
Human (Maynard et al. 2021)
Healthy DLPFC
3 donors
12 sections
Mouse (Hasel et al. 2021)
Healthy + Inflamed Whole Hemisphere
Healthy (n = 3)
Inflamed (n = 3)
10X Visium Spatial Transcriptomics
Our Astrocyte snRNA-seq Data
Cluster marker genes
Cluster Gene Modules
Spatial Gene Expression Resolution Enhancement (BayesSpace)
Calculate Spot-level Gene Module Scores
Calculate Subspot-level Enrichment Scores
Regional Differential Enrichment Testing
Plot Spatial Enrichment Scores
Visualization
Differential Enrichment Testing
B
CLUSTER 6 GENE MODULE
H&E
Spot-level Gene Module Score
Resolution-Enhanced Enrichment Score
Gene Module Score
Relative Enrichment
Min
Max
C
White Matter Annotation
WM Score
White Matter
Gray Matter
D
Final Region Annotation
UMAP2
UMAP1
L1
L2/3
L4
L5
L6
WM
E
ρ
F
zH
Cluster 1
Cluster 6
Cluster 0
Cluster 8
Cluster 5
Cluster 3
Cluster 2
Cluster 4
Cluster 7
G
Relative Enrichment
Min
Max
CLUSTER 0
CLUSTER 1
CLUSTER 2
CLUSTER 3
CLUSTER 4
CLUSTER 5
CLUSTER 7
Gene Module Score
H
= Saline
= LPS
AD-ASSOCIATED GENE MODULES
Cluster 0
Cluster 1
Cluster 2
Cluster 3
Cluster 4
Cluster 6
Cluster 7
Cluster 8

Figure S12 (related to Figure 6). Localizing heterogeneous astrocyte gene signatures across the human and mouse cortex. **(A)** Schematic overview of analysis pipeline used to explore enrichment of cluster-specific astrocyte gene sets across human and mouse cortex. Maynard et al. (2021) data is from post-mortem human dorsolateral pre-frontal cortex (DLPFC) with no noted pathology (3 donors, n = 12 sections). Hasel et al. (2021) data from mice injected with saline or lipopolysaccharide to induce inflammation (n = 3 per condition). 10X Chromium Visium data from each dataset was visualized and tested for differential enrichment across cortical regions using parallel method (see Methods). **(B)** Spot-level gene module scores (middle) and resolution-enhanced enrichment scores (right) for astrocyte Cluster 6 gene set overlaid on a representative section from the Maynard et al. (2021) data, illustrating the Bayesian resolution enhancement method used for improved visualization. **(C)** White matter gene expression score (WM score) overlaid on a representative mouse brain section from Hasel et al (2021), and density plot of WM score across all six sections. Dotted line indicates threshold used to annotate spots as white matter or gray matter. **(D)** (left) tSNE plot of Hasel et al (2021) Visium spots colored by final region annotation. (right) Representative section overlaid with final spot regional annotations. **(E)** Spearman correlations between human cortical regions and mouse cortical regions. Correlations were performed using scaled average expression of all one-to-one orthologous genes that were highly variable in both datasets (707 genes). **(F)** Heatmap of z-scored Kruskal-Wallis test statistic H, testing differential enrichment of each cluster gene module across cortical regions in each dataset. All cluster gene modules were significantly differentially enriched across regions (Kruskal-Wallis test with Bonferroni correction, $p < 0.05$). Z-scored test statistics illustrate the degree to which gene module scores differ across cortical regions in each dataset. **(G)** Visualization and differential enrichment results for each astrocyte cluster (top: human; bottom: mouse). (left) Relative enrichment of cluster gene module across representative Visium section. (right) Box and density plot of gene module scores across all spots and all sections grouped by cortical region. +/- symbol represents whether the cluster gene module is significantly enriched or de-enriched, respectively, in spots from the indicated region compared to the rest of the cortex (Wilcoxon rank sum test with Bonferroni correction). **(H)** Box & density plots comparing expression of modules of genes that were upregulated in AD in each astrocyte cluster in our snRNA-seq data across spots in various cortical regions in saline versus LPS-injected mice. +/- symbol represents whether the AD gene module is significantly upregulated or downregulated, respectively, in spots from the indicated region in LPS versus saline-injected mice (Wilcoxon rank sum test with Bonferroni correction). See **Table S7** for exact test statistics and p-values.

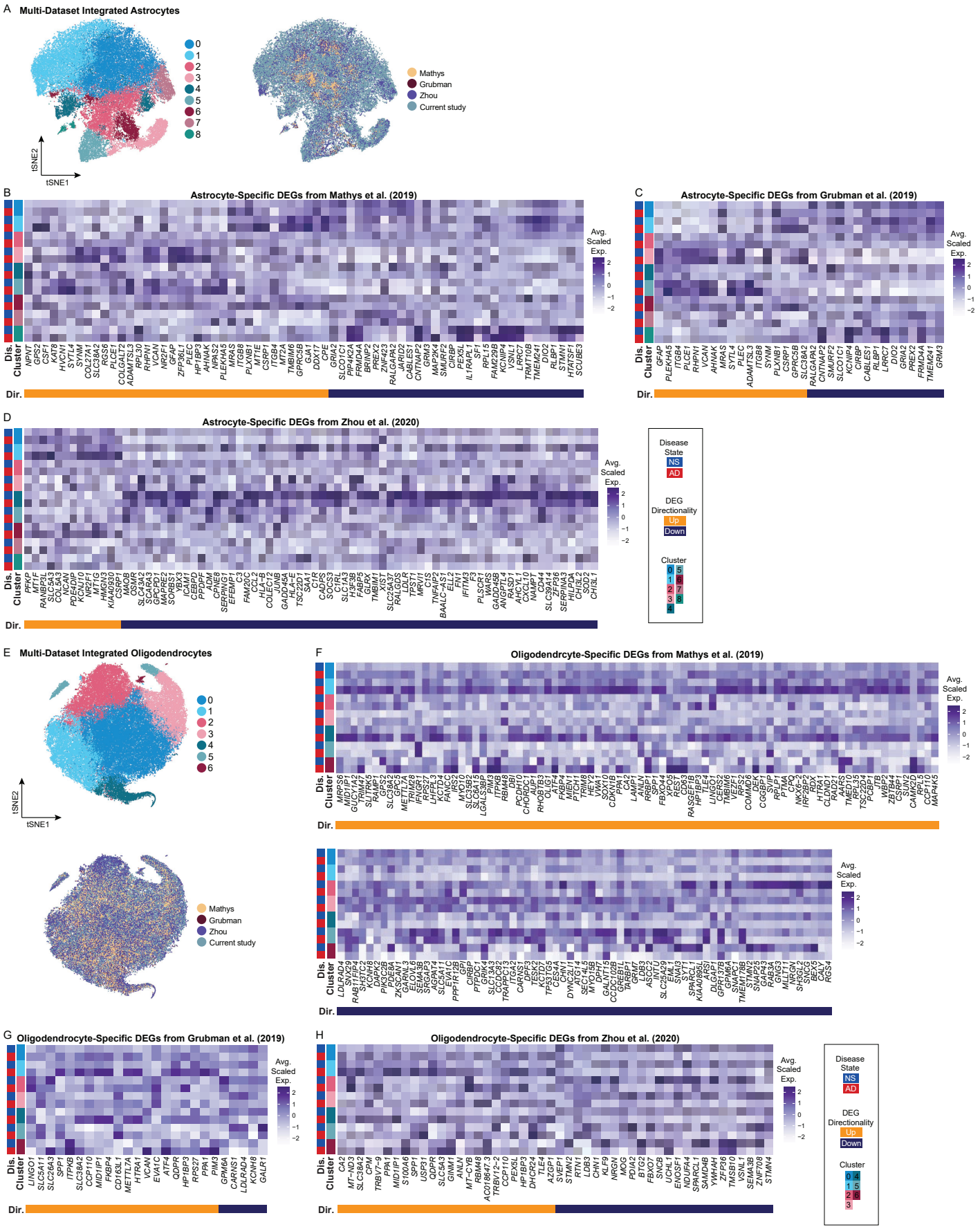

Figure S13 (related to Figures 3,7). Probing integrated astrocyte and oligodendrocytes for previously published Alzheimer's associated differentially expressed genes. (A) tSNE plots of integrated astrocytes as visualized by cluster (left) and by dataset (right). Mathys data are in yellow, Grubman data are in dark red,

Zhou data are in violet, and the current study's data are in steel blue. Heatmaps of differentially expressed genes (DEGs) from Mathys et al. 2019 **(B)**, Grubman et al. 2019 **(C)**, and Zhou et al. 2020 **(D)**. Alzheimer's-associated DEGs in the Zhou et al. dataset were detectable in the integrated dataset (upregulated – cluster 5; downregulated cluster 2), likely due to increased numbers of sequenced astrocytes. Other reported disease-associated astrocyte DEGs were not specific to individual clusters. Conversely, reverse-probing for previously described disease-associated oligodendrocyte cluster-specific DEGs was more successful. **(E)** tSNE plots of integrated oligodendrocytes as visualized by cluster (left) and by dataset (right). Mathys data are in yellow, Grubman data are in dark red, Zhou data are in violet, and the current study's data are in steel blue. **(B-D)** Heatmaps of disease-associated DEGs from each dataset attributed to oligodendrocytes. **Abbreviations:** AD, Alzheimer's disease; DEG, differentially expressed gene; Dir., direction; Dis., disease; F, female; M, male; NS, non-symptomatic.